Biogeosciences Discuss., 11, 8635–8672, 2014
www.biogeosciences-discuss.net/11/8635/2014/
doi:10.5194/bgd-11-8635-2014
© Author(s) 2014. CC Attribution 3.0 License.

Biogeosciences
Discussions
Open Access

This discussion paper is/has been under review for the journal Biogeosciences (BG).
Please refer to the corresponding final paper in BG if available.

Oxygen and carbon isotope composition of modern planktic foraminifera and near-surface waters in the Fram Strait (Arctic Ocean) – a case-study

T. Pados[1], R. F. Spielhagen[1,2], D. Bauch[1], H. Meyer[3], and M. Segl[4]

[1]GEOMAR Helmholtz Centre for Ocean Research Kiel, Kiel, Germany
[2]Academy of Sciences, Humanities, and Literature Mainz, Mainz, Germany
[3]Alfred Wegener Institute Helmholtz Centre for Polar and Marine Research, Potsdam, Germany
[4]MARUM – Center for Marine Environmental Sciences, Bremen, Germany

Received: 14 May 2014 – Accepted: 19 May 2014 – Published: 11 June 2014

Correspondence to: T. Pados (tpados@geomar.de)

Published by Copernicus Publications on behalf of the European Geosciences Union.

Abstract

The upper 500 m of the water column and the sediment surface along an E–W transect in the Fram Strait were sampled for recent planktic foraminifera. The δ^{18}O and δ^{13}C values of the tests are compared to the stable isotope composition of water samples taken from the same depths, and related to the characteristics of the water column. The polar species *Neogloboquadrina pachyderma* (sin.) clearly dominates the species assemblage in the Fram Strait in the early summer, while the subpolar *Turborotalita quinqueloba* accounts only for 5–23 %. In this area the average depth of calcification of *N. pachyderma* (sin.) lies between 70–150 m water depth, *T. quinqueloba* shows a similar range with 50–120 m water depth. The δ^{18}O values of *N. pachyderma* (sin.) show an average vital effect of about −1.5 ‰ compared to calculated equilibrium calcite values. Except for the upper ~ 75 m, the vertical profiles of δ^{13}C of the net-sampled shells are nearly parallel to the values measured in the water column with an average offset of −1.6 ‰ and −3.6 ‰ for *N. pachyderma* (sin.) and *T. quinqueloba*, respectively. The discrepancy found in the upper ~ 75 m might indicate the influence of the "carbonate ion effect" on the carbon isotope incorporation in the tests. Oxygen and carbon isotopes from the sediment surface yield higher values than those from the water column for both species. This may be because specimens from the water column reflect a modern snapshot only, while tests from surface sediments record environmental parameters from the past ~ 1000 years.

1 Introduction

The stable isotope composition of foraminiferal shells from sediment cores is often used in palaeoceanographic studies to reconstruct past oceanic environments. Planktic foraminifera precipitate their calcite tests from the surrounding seawater. Thus, variations in the stable oxygen (^{18}O/^{16}O, δ^{18}O) and stable carbon (^{13}C/^{12}C, δ^{13}C) isotope ratios of shell carbonate should reflect variations of the stable isotope compo-

cc BY

sition of the ambient water. This, on the other hand, is determined by the interplay of various factors (e.g., evaporation, sea-ice formation, productivity). Therefore, δ^{18}O values of fossil planktic foraminiferal shells have been widely used to estimate sea surface temperatures (e.g., Kellogg et al., 1978; Erez and Luz, 1983), salinity (e.g., Duplessy et al., 1992), and ocean stratification (Simstich et al., 2003). Planktic δ^{13}C records are generally assumed to reflect changes in paleoproductivity and ventilation of surface and near-surface waters (Duplessy, 1978). Several studies of living planktic foraminifera showed that these protozoa do not calcify in equilibrium with the ambient sea water (Shackleton et al., 1973; Vergnaud Grazzini, 1976; Kahn, 1979; Kohfeld et al., 1996; Bauch et al., 1997; Volkmann and Mensch, 2001) and that the stable isotope composition of their tests is influenced not only by regional effects but also by numerous other chemical (e.g., pH, carbonate ion concentration) and biological (e.g., symbiont photosynthesis, metabolic activity, test weight) factors. Increasing pH and carbonate ion concentrations are known to decrease stable isotope ratios (Spero et al., 1997; Bauch et al., 2002), while the presence of symbionts causes depletion in ^{18}O and an increase in δ^{13}C values of the shells (Spero and Deniro, 1987). A higher metabolic rate, characteristic for earlier ontogenetic stages (Hemleben et al., 1989), is associated with a discrimination against heavy isotopes (McConnaughey, 1989). Furthermore, planktic foraminifera are assumed to migrate in the water column during ontogeny (Berberich, 1996; Schiebel and Hemleben, 2005) and form their secondary calcite crust while descending into deeper layers (Simstich et al., 2003). Heavier, encrusted individuals are reported to have higher δ^{18}O and lower δ^{13}C values (Kohfeld et al., 1996; Bauch et al., 1997; Volkmann and Mensch, 2001; Simstich et al., 2003). Combinations of these and other factors make the fossil record difficult to interpret. For example, while both increasing temperature and symbiont activity tend to decrease the δ^{18}O value, at the same time both of them can increase the test weight (Hecht, 1976; Spero, 1992), and thereby also indirectly increase the ^{18}O / ^{16}O ratio. Thus, it is essential for an improved interpretation of isotopic records from sediment cores to have detailed knowledge on how modern environmental parameters influence the stable isotope composition of living foraminifera and to which degree the isotopic composition of their shells reflects the composition of the ambient sea water.

Here we report on results from a multidisciplinary approach to investigate the effects of environmental factors on the isotopic composition of polar planktic foraminifera. Our study was performed in the Fram Strait that connects the Arctic and North Atlantic Oceans and comprises strong oceanographic contrasts (Fig. 1). On an E–W transect between the Svalbard and Greenland margins, the upper water column and sediment surface were sampled for planktic foraminifera species *Neogloboquadrina pachyderma* (sinistral) (Ehrenberg, 1861) and *Turburotalita quinqueloba* (Natland, 1983). The stable oxygen and carbon isotope compositions of net-sampled tests are compared to the isotope data of ambient seawater and to that of tests from sediment surface samples. Possible reasons for the revealed discrepancies are discussed. Findings about the species assemblage and depth distribution of foraminifera from the same samples are discussed in Pados and Spielhagen (2014).

2 Hydrographical setting

The Fram Strait is the only deep passage between the Arctic Ocean and the rest of the world ocean, supplying the Arctic Ocean with waters of North Atlantic origin. The oceanography is dominated by two major surface current systems: the northward flowing West Spitsbergen Current (WSC) carries warm and saline water masses, while in the East Greenland Current (EGC) cold and fresh Polar waters exit the Arctic Ocean (Johannessen, 1986). The upper 500 m of the WSC are dominated by Atlantic Water (Rudels et al., 1999), characterized by temperatures higher than 0.5 °C and salinities above 34.5 (Jones, 2001). In the western part of the strait the upper 200 m are characterized by temperatures below 0 °C and salinities between 32 and 34. In the summer, as a result of ice melt, the surface waters have even lower salinities (below 32). A well-developed halocline separates the Polar waters from the Atlantic Layer found between 200 and 500 m (Rudels et al., 2000). The interaction between these two water masses

CC BY

controls the sea-ice coverage in the strait. In summer the ice cover usually extends from Greenland to the East Greenland shelf edge but it can intrude also into the eastern part of the strait in the case of extremely cold winter/spring conditions (Dickson et al., 2000).

The oceanographic system is highly variable and the surface distribution of Polar waters can change on a daily timescale (e.g. Beszczynska-Möller et al., 2011). Oceanographic measurements during cruise ARK XXVI/1 (Beszczynska-Möller and Wisotzki, 2012) provide a detailed profile across the Fram Strait at the time of sampling (Fig. 2). The upper 500 m of the WSC were characterized by salinities near 35 and temperatures between 4 °C and 2 °C. At the surface an approx. 100 m thick, warm layer was observed, with temperatures up to 7–8 °C. During the time of sampling, at stations 35 and 39, cold and fresh water masses intruded into the upper 50–100 m of this layer. After one week these water masses were not present anymore at the same locations (see water column properties at 3° E (station 87) that was sampled 8 days later), in agreement with high variability of oceanic fluxes in this region (Beszczynska-Möller et al., 2011). In the western part of the strait and in the EGC, the Polar waters extended down to ~ 200 m water depth and had salinities around 33 and an average temperature of −1.5 °C at the time of the sampling (Fig. 2). Here, on the very surface low salinities (~ 30) were found that is probably caused by melt water. The Polar waters were mainly ice-covered. Below ~ 200 m water depth submerged warmer and salty Atlantic waters were found. The sea-ice margin over the position of the transect was located at ~ 2° W during the sampling period.

3 Material and methods

Plankton tow, sediment surface and water samples used in this study were obtained during expedition ARK XXVI/1 with research vessel *Polarstern* in June/July 2011 in the Fram Strait. Samples were collected at 10 stations along a transect at 78°50′ N across the Fram Strait (Fig. 1, Table 1). Plankton samples were collected by a MultiNet sampler (net opening 0.5 m^2, Hydro-Bios, Kiel, Germany); the nets of 63 µm mesh size were towed vertically on regular depth intervals (500–300 m, 300–200 m, 200–100 m, 100–50 m, 50–0 m). Sediment surface samples were obtained from multicorer deployments at the same stations. Sample collection and handling procedures are described in detail by Pados and Spielhagen (2014).

For stable isotope analysis 10–25 specimens of *N. pachyderma* (sin.) and 10 specimens of *T. quinqueloba* were picked from the > 100 µm fraction (plankton samples) and from the 100–250 µm fraction (sediment samples). The number of picked tests was restricted by the number of available, same-sized and clearly identifiable shells. The oxygen and carbon isotope analysis was performed at the GEOMAR Stable Isotope Lab using a Finnigan-MAT 253 mass spectrometer system connected to a Kiel IV Carbonate Preparation Device.

Temperature and salinity of the water column were measured by a conductivity-temperature-depth (CTD) profiler (Beszczynska-Möller and Wisotzki, 2012), immediately before the deployment of plankton tows. Data of ice coverage were obtained by shipboard observations. Water samples for stable isotope analyses were taken from the rosette sampler, immediately after arriving on the deck to minimize the exchange of contained CO_2 with the atmosphere. Water samples for $\delta^{13}C$ analysis (100 mL) were drafted carefully into glass bottles without sputtering and thus avoiding bubbles. Samples were immediately poisoned with $HgCl_2$ (0.2 mL) to stop biochemical reactions, which may alter the carbon isotopic composition of CO_2, and bottles were then sealed by aluminium caps with high-density butyl-rubber plugs. Water samples for $\delta^{18}O$ analysis (50 mL) were filled into glass bottles and sealed by plastic screw-on caps. The oxygen and carbon isotope mass ratios of the water samples were measured in the stable isotope laboratories of AWI Potsdam with a Finnigan-MAT Delta-S mass spectrometer with two coupled equilibration units ($\delta^{18}O$) and of MARUM (Bremen) using a Gasbench coupled to a MAT 252 mass spectrometer ($\delta^{13}C_{DIC}$), with a precision and accuracy of at least ±0.1 ‰ and ±0.15 ‰ for $\delta^{18}O$ (Meyer et al., 2000) and $\delta^{13}C_{DIC}$, respectively.

cc BY

"Equilibrium calcite values" (δ_c) were calculated for the water samples between sea surface and 500 m water depth from actual δ^{18}O (δ_w) and temperature (T) measurements according to the so called "palaeotemperature equation" of O'Neil et al. (1969):

$$T = 16.9 - 4.38(\delta_c - \delta_w) + 0.1(\delta_c - \delta_w)^2 \quad (1)$$

where δ_c and δ_w are the stable oxygen isotope values of the calcite and the water on the PDB scale, respectively. Isotope measurements of water are presented using SMOW as a standard. δ^{18}O (SMOW) was converted to δ^{18}O (PDB) for the palaeotemperature equation according to Bemis et al. (1998):

$$\delta^{18}\mathrm{O(PDB)} = 0.9998\delta^{18}\mathrm{O(SMOW)} - 0.2\,‰. \quad (2)$$

Weighted averages of the stable isotope results for each station were calculated using the standing stock (sum of isotope values for each interval multiplied with the concentration of foraminifera in depth interval/sum concentrations in all intervals; see Bauch et al., 1997).

4 Results

4.1 Water column properties

4.1.1 Stable isotopes in the upper water column

In general, oxygen isotope composition of water is roughly linearly correlated to salinity (Fig. 3). Both change along the transect with lowest values at the surface and are continuously increasing with depth. Surface δ^{18}O and salinity are lowest in the west and highest in the east (Fig. 4). The vertical δ^{18}O profiles of the two westernmost stations show strong similarities with the vertical profiles of stations 35 and 39 (4° E

cc BY

and 2° E, respectively) where during the time of sampling cold and fresh water masses intruded into the warm surface waters. At these four stations extremely low salinity and δ^{18}O values mark Polar waters at the surface that are reaching from the surface down to ~ 200 m water depth at stations 75 and 71 and to ~ 100 m water depth at stations 39 and 35. Below the surface layers the Atlantic waters are characterized by relatively high and constant δ^{18}O values of about +0.3 ‰ (Fig. 4). The remaining six stations reveal more scatter: we found a slight increase from the surface to 25 m water depth, then a decrease to 75–100 m depth, followed by homogeneous δ^{18}O values of the Atlantic Layer (Table 2). When evaluating average values over the upper 500 m of water column, the two westernmost stations (75 and 71) yield the lowest average values (−0.41 ‰, ±0.94 and −0.84 ‰, ±1.16, respectively) while the highest average value (+0.34 ‰, ±0.03) is observed at 3° E at station 87.

The vertical variation of the carbon isotope composition of the dissolved inorganic carbon (DIC) in the upper 500 m of the water column is rather small. The $\delta^{13}C_{DIC}$ values have an average value of about +1.04 ‰ with a standard deviation of 0.24. Surface waters always yield heavier values, decreasing down to ~ 100 m water depth followed by relatively constant values down to 500 m water depth (Fig. 4, Table 2).

4.1.2 Equilibrium calcite values

The equilibrium calcite values calculated from δ^{18}O and temperature of seawater increase constantly with depth in the eastern part of the strait, while at stations 71 and 75, in the western part of the strait, a stronger increase is observed from the surface down to 150 m water depth, followed by a slight decrease. A similar pattern, though in a narrower range, can be found at stations 35 and 39, in the middle of the strait, where near the surface unusually low temperatures of the water were recorded during the sampling period (Fig. 7, Table 2).

4.2 Species distribution of planktic foraminifera

In the Fram Strait the planktic foraminiferal fauna is dominated by polar species *Neogloboquadrina pachyderma* (sinistral coiling) and subpolar symbiont bearing *Turborotalita quinqueloba* (Volkmann, 2000; Simstich et al., 2003; Pados and Spielhagen, 2014). *N. pachyderma* (sin.) clearly prevails in our samples contributing to the total assemblages with 73–92 % compared to the the subpolar *T. quinqueloba*, contributing with 23–5 %. The proportion of *N. pachyderma* (sin.) shows an increasing trend towards the west while *T. quinqueloba* follows an exactly reverse tendency. Both species have maximum absolute abundances between 0–100 m water depth with a shallower maximum under the ice cover than in the open ocean (Figs. 5 and 6). The species assemblage found in the sediment surface was found to correlate best with the living fauna caught between 50–100 m water depth (Pados and Spielhagen, 2014).

4.3 Stable isotope composition of foraminifera

4.3.1 *Neogloboquadrina pachyderma* (sin.)

The oxygen isotope composition of *N. pachyderma* (sin.) from sediment surface samples shows lowest values at the three easternmost stations (stations 127, 25, 19; at 8–6° E). The highest value is found in the western part at station 75, at 4° W. The sediment surface samples have an average δ^{18}O value of +3.2 ‰ (±0.3) (Table 3). The plankton samples generally have a lower oxygen isotope composition than the sediment surface samples. The weighted average δ^{18}O values at each station are ranging from −0.7 ‰ to +3.3 ‰ over the whole transect. There is no clear east-west difference and the stations in the middle of the strait (stations 35, 39 and 54) yield the highest values. The vertical distribution of δ^{18}O does not show a well-pronounced trend. The only clearly recognizable pattern is that values in the depth interval of 0–50 m are usually lower than those from the interval 50–100 m (an exception is station 54 where the surface waters yielded slightly heavier δ^{18}O values) (Fig. 7, Table 4).

The $\delta^{13}C$ values of *N. pachyderma* (sin.) from sediment surface samples are relatively constant and have an average value of +0.5 ‰ (±0.2). The lateral distribution of the $\delta^{13}C$ values from the sediments shows a trend similar to the $\delta^{18}O$ results: the easternmost stations (stations 127, 25, 19; at 8–6° E) have the lowest values while the highest are found in the western part of the section, at the sea ice margin at 2° W (Table 3). The carbon isotope composition of *N. pachyderma* (sin.) from plankton tows shows lower values at each station than the $\delta^{13}C$ values from sediments. The $\delta^{13}C$ values of plankton samples have a mean of −0.8 ‰ (±0.7) of weighted averages over the whole transect. The plankton samples do not follow the E–W trend found in the core top samples and both the lowest and the highest values are found at stations in the middle of the transect (stations 87 and 39, respectively). Vertical $\delta^{13}C$ profiles of the plankton samples show increasing values from the sea surface down to the depth interval of 100–200 m (exceptions are stations 127, 87 and 71 where maximum values lie in the depth interval of 50–100 m), followed by a slight decrease to 300–500 m (Fig. 7, Table 4).

4.3.2 *Turborotalita quinqueloba*

Both oxygen and carbon isotope compositions of *T. quinqueloba* from sediment surface samples show increasing values from east to west; averaging over the transect −0.1 ‰ (±0.2) and +2.7 ‰ (±0.3), respectively (Table 3).

The weighted average of the $\delta^{18}O$ and $\delta^{13}C$ values of net sampled specimens scatter along the stations and do not show any pronounced east-west difference. The vertical profiles of both parameters show extremely low values near the surface compared to all other depth intervals. The vertical variation of the $\delta^{18}O$ and $\delta^{13}C$ values in *T. quinqueloba* is much bigger than the variation found in *N. pachyderma* (sin.) (Fig. 8, Table 4). However, it has to be taken into account that the number of specimens available for isotope analysis (on average ten tests) was rather low and possibly not sufficient to yield reliable results for this thin-walled species. We cannot exclude that the differences in variation are due to a non-systematic error in the isotope measurements of *T. quinqueloba*.

5 Discussion

5.1 Oxygen isotope values of water samples and foraminifera

The calculated equilibrium calcite isotope composition represents the theoretical δ^{18}O value of inorganic calcite precipitated in isotopic equilibrium with the surrounding seawater. The offset found between the equilibrium calcite value and the measured δ^{18}O value of foraminiferal tests is commonly described as "vital effect" related to differential isotopic uptake in carbonate organisms compared to equilibrium conditions. The δ^{18}O values of living foraminifera in our work area during early summer were consistently lower than the calculated equilibrium calcite values. The mean offsets were −1.5 ‰ in *N. pachyderma* (sin.) and −3.7 ‰ in *T. quinqueloba*. Based on previously published results, the magnitude of the vital effect in *N. pachyderma* (sin.) appears to vary regionally. Bauch et al. (1997) reported a consistent offset of −1.0 ‰ between equilibrium calcite values and δ^{18}O data of net-sampled *N. pachyderma* (sin.) in the Nansen Basin. Volkmann and Mensch (2001) found an average vital effect of −1.3 ‰ in the Laptev Sea for *N. pachyderma* (sin.) and −1.6 ‰ and −1.3 ‰ in the Fram Strait for *N. pachyderma* (sin.) and for *T. quinqueloba*, respectively. Plankton tows from various hydrographic regimes in the Nordic Seas revealed vital offsets of −1.0 ‰ and −1.1 ‰ for *N. pachyderma* (sin.) and *T. quinqueloba*, respectively (Simstich et al., 2003). Significantly smaller offsets were reported from the western subpolar North Atlantic, calculated from shells collected with sediment traps (Jonkers et al., 2010).

In our study *T. quinqueloba* shows larger offsets between the equilibrium calcite values and the measured δ^{18}O values than *N. pachyderma* (sin.). Earlier works (e.g., Fairbanks et al., 1980; Lončariċ et al., 2006) also recorded a larger negative offset in spinose species compared to nonspinose species. Moreover, symbiont-containing species, like *T. quinqueloba*, are known to be more depleted in ^{18}O as a consequence of higher CO_2 fixation caused by photosynthesis (Bijma et al., 1990; Spero et al., 1997). In *N. pachyderma* (sin.) we found a clear east-west difference in the magnitude of the vital effect along the transect, similar to observations by Volkmann and Mensch (2001). In their study the eastern and western part of the strait yielded significantly different offsets, with highest deviations from the equilibrium calcite values in the west. They concluded that ice coverage increases the magnitude of the vital effect. In our samples in *N. pachyderma* (sin.) the strongest disequilibrium was indeed found at the two ice-covered stations (−4.0 ‰ and −1.8 ‰, at 4° W and 5° W, respectively) and at station 87 (−3.9 ‰, at 4° E). These results are also in line with observations of Bauch et al. (1997) who found slightly increasing isotopic differences between water and plankton samples with decreasing salinity and temperature. Volkmann and Mensch (2001) explained the greater vital offset in the cold and less saline waters of the western Fram Strait with faster growth and consequently higher calcification rates caused by unfavourable conditions. An increased calcification rate decreases the δ^{18}O of tests (McConnaughey, 1989) and may thus increase the disequilibrium. While this hypothesis can explain high offsets at increased calcification rates, the validity of the hypothesis seems rather unlikely as unfavourable conditions generally lead to lower metabolism and thus, decreased calcification rates. Moreover, lower temperatures decrease metabolic rates in all organisms (Hemmingsen, 1960; Gillooly et al., 2001). The abrupt increase in the offset close to the sea-ice margin may rather be explained by increased primary production, associated with the ice margin. During biological production dissolved inorganic carbon is consumed and this considerably increases pH and consequently the carbonate ion concentration ($[CO_3^{2-}]$) of the water (Chierchi and Franson, 2009). Spero et al. (1997) showed that increasing seawater $[CO_3^{2-}]$ decreases the $^{18}O/^{16}O$ ratios of the shells of foraminifera and may thus simultaneously increase the vital effect. Still, the effect of carbonate ion concentrations alone cannot explain the high deviation from equilibrium calcite found at station 87 where no increased primary production is expected. A possible reason for the increased vital effect at stations 71, 75 and 87 might also be a sampling during different ontogenetic stages. *N. pachyderma* (sin.) is known to reproduce on a synodic lunar cycle (Bijma et al., 1990; Schiebel and Hemleben, 2005) and as these three stations were sampled in sequence in the second half of the cruise, it is possible that in the respective samples there were more specimens in early life stages compared to the stations sampled 7–10 days before. Early ontogenetic stages are associated with higher respiration and calcification rates (Hemleben et al., 1989). Rapidly growing skeletons tend to show depletion in both ^{13}C and ^{18}O (McConnaughey, 1989), which could account for the increased vital effect observed at the respective stations.

In contrast to *N. pachyderma* (sin.), the offsets found between equilibrium calcite values and the δ^{18}O values of *T. quinqueloba* do not follow a clear trend along the transect and show great scatter (Fig. 8). However, the low numbers of specimens found in the samples at most of the stations did not allow us to determine δ^{18}O over the whole water column sampled. Moreover, as a consequence, lower numbers of tests (on average ten) were used for stable isotope analysis than in *N. pachyderma* (sin.) (25), which might also account for the scatter in both δ^{13}C and δ^{18}O values in *T. quinqueloba*. We therefore refrain from discussing the vital effect in *T. quinqueloba*.

Our analysis shows that recent specimens of planktic foraminifera from the water column have a lower oxygen isotopic value than fossils on the sediment surface (Figs. 7 and 8). This is in agreement with a number of studies conducted in different regions of the world (e.g., Duplessy et al., 1981; Schmidt and Mulitza, 2002). Berger (1970) suggested in his hypothesis on intraspecific selective dissolution that within one species preferentially the thin-shelled individuals are dissolved during deposition. These tests are secreted during the warmest period of the year and thus, their dissolution increases the average δ^{18}O value of the species in the core top samples. In the Nordic Seas the production maximum of planktic foraminifera occurs during summer (Kohfeld et al., 1996; Jonkers et al., 2010), with almost zero production during other seasons. This means that the majority of the specimens calcifies the shells under similar conditions. Accordingly, differences in the thickness of tests are not to be expected. Therefore the hypothesis of Berger (1970) cannot explain the isotopic differences between plankton and sediment surface samples in this region. Lateral transport of the shells during deposition is another effect that could explain the discrepancies. However, mean transport distances in the Fram Strait are only 25–50 km for *N. pachyderma* (sin.) and 50–100 km for *T. quinqueloba* (von Gyldenfeldt et al., 2000). These distances are too short to transport isotopic signatures from water masses with significantly different temperature/salinity signatures into the sediments. The offset found in the δ^{18}O values between plankton and sediment surface samples can be attributed rather to the age difference between living plankton and sediment surface samples. Core top samples are assumed to represent modern conditions in palaeoceanographic reconstructions. Nevertheless, depending on sedimentation rates and bioturbation intensity, their average age can vary in a great range (in the Fram Strait a few decades to 3 ky, on average 1 ky, see Simstich et al., 2003) while net-sampled foraminifera reflect a snapshot of actual modern conditions. Discrepancies found between isotopic composition of shells collected on the sediment surface and in the water column may therefore be related to changes in the oceanographic parameters between the early summer of 2011 and average conditions during the period represented by sediment surface samples. To explain the lower modern δ^{18}O values, the water mass in the calcification depth interval of the foraminifera must have become warmer and/or the $\delta^{18}\mathrm{O}_{\mathrm{water}}$ must have decreased and thus, the salinity signature must have changed significantly. Both rising temperatures and increasing river discharges have been documented for the last decades in the Arctic (e.g., Zhang et al., 1998; Serreze et al., 2000; Peterson et al., 2002; Spielhagen et al., 2011). The mean offset found between the δ^{18}O values of net-sampled foraminifera and the tests from the sediment surface along the transect is ~ 1.3 ‰. Assuming that the oxygen isotope composition of the water remained constant over the time, this difference would correspond to a change in water temperature of about 5 °C. Neglecting the two extremely high offsets found at stations 75 and 87, the mean offset would decrease to ~ 0.6 ‰, corresponding to a temperature change of ~ 2.4 °C. A temperature change of 2.4 °C is similar to the reconstructed temperature increase of Atlantic Water during the last 200 years (Spielhagen et al., 2011). However, a temperature change of 5 °C during the last millennia over the whole Fram Strait area seems much too large and clearly, water temperature changes may not solely account for the differences found in the isotopic composition between modern and fossil foraminifera. The results nevertheless suggest the combined effect of temperature rise and $\delta^{18}O_{water}$-change, possible dissolution and transport effects during the last ~ 1000 years.

5.2 Calcification depth

With currently available methods we cannot directly determine the actual calcification depth of planktic foraminifera in the water column. Therefore we assume that planktic foraminifera build their shells at the depth where they are most abundant. The average depth of calcification (calculated from the standing stock) of *N. pachyderma* (sin.) in the Fram Strait lies between 70–150 m water depth. *T. quinqueloba* shows a similar calcification range at 50–120 m water depth (Figs. 5 and 6). Both species show deepest average calcification depth at the easternmost station. Our results are in accordance with Simstich et al. (2003) who calculated an apparent calcification depth for *N. pachyderma* (sin.) of 70–130 m and 70–250 m in the EGC and off Norway, respectively. From the Nansen Basin (eastern Arctic Ocean), Bauch et al. (1997) reported a deeper average calcification depth for *N. pachyderma* (sin.). However, in the northern regime of the Nansen Basin, where the water column properties are similar to those in the western Fram Strait, *N. pachyderma* (sin.) prefers shallower waters than in the southern Nansen Basin where the water column is strongly influenced by the subsurface inflow of Atlantic Waters (Bauch et al., 1997). This trend observed by Bauch et al. (1997) coincides with our results. The difference found in calcification depths in the Nansen Basin and in the Fram Strait might be caused by the different habitats that these locations represent. The northern Nansen Basin is covered by sea ice throughout the year and thus represents a different habitat for planktic foraminifera compared to the narrow Fram Strait. Here, the interannual W–E variability in the position of the average summer sea ice margin is high and the ice-covered stations sampled in this study might therefore be ice-free in another summer. It has been shown that the depth habitat of planktic foraminifera in the Fram Strait in the early summer is predominantly controlled by the position of the deep chlorophyll maximum (Pados and Spielhagen, 2014). The permanent ice cover in the Nansen Basin may alter the factors controlling the depth habitat of foraminifera and may consequently cause a different depth habitat (and calcification depth) than in the Fram Strait.

Calculating the vital effect from differences between water and plankton samples at each depth level assumes that foraminifera calcified their tests at the depth interval where they were caught. This might not be true, as foraminifera are known to migrate in the water column during their life cycle. Alternatively we may assume that the main encrustation process of foraminifera indeed happened solely at the average calcification depth that is derived in our study from the standing stock. When calculating the average offset between water and foraminifera for the calcification depth only, a vital effect of −0.9 ‰ in *N. pachyderma* (sin.) and −3.1 ‰ in *T. quinqueloba* is determined. These vital effects are significantly smaller than those determined over the whole water column, which are −1.5 ‰ and −3.7 ‰ for *N. pachyderma* (sin.) and *T. quinqueloba*, respectively. In general, we have to take into account that both calcification-scenarios represent extreme cases and the actual vital effect may be between these two extremes.

5.3 Carbon isotope values of DIC and foraminifera

The interpretation of the carbon isotope composition of foraminiferal shells is quite complicated as several factors can influence the carbon isotope incorporation. The gas exchange between sea and atmosphere, the biological production, the community respiration and species dependent incorporations of carbon isotopes are the main processes that can affect the $^{13}C/^{12}C$ ratio in calcite tests. A number of studies reported on a consistent offset between $\delta^{13}C$ of calcite shells and the $\delta^{13}C_{DIC}$ measured within the water column (e.g., Bauch et al., 2000; Volkmann and Mensch, 2001). According to

CC BY

Romanek et al. (1992) δ^{13}C of inorganic calcite that precipitates in equilibrium with seawater is 1 ‰ higher than $\delta^{13}C_{DIC}$. In our study area below 75 m water depth the δ^{13}C values of *N. pachyderma* (sin.) run relatively parallel to the $\delta^{13}C_{DIC}$, but with an average offset of −1.6 ‰. This reveals a vital effect of about −2.6 ‰. Kohfeld et al. (1996) reported from the Northeast Water Polynya on the Greenland shelf a vital effect of −1 ‰ while another study in the Nansin Basin (Bauch et al., 2000) revealed a vital effect of −2 ‰. The discrepancies found here may suggest the influence of oceanographic variability on the vital effect in δ^{13}C of *N. pachyderma* (sin.). The δ^{13}C of *T. quinqueloba* shows a stronger vertical scatter with an average vital effect of −4.6 ‰. However, in the upper 75–100 m of the water column for both species the $\delta^{13}C_{DIC}$ and the δ^{13}C of shells show an exactly reverse tendency (Figs. 7 and 8). The high $\delta^{13}C_{DIC}$ values found close to the sea surface are assumed to be caused by high primary production, resulting in enrichment in ^{13}C (Fogel and Cifuentes, 1993): as ^{12}C is taken for photosynthesis, the water becomes enriched in ^{13}C. However, if no other processes would affect the incorporation of carbon into the calcite shells, the tests should also show the enrichment in ^{13}C. One possible explanation for the deviation might be an increased carbonate ion concentration ($[CO_3^{2-}]$) as a consequence of strong biological production in the upper water column (Chierchi and Franson, 2009). Both culturing (Spero et al., 1997) and field experiments (Bauch et al., 2002) have shown that the carbon isotope composition of foraminifera is correlated to the carbonate ion concentration of the water. The “carbonate ion effect” (CIE) describes that increasing seawater $[CO_3^{2-}]$ causes depletion in ^{13}C of the foraminiferal tests. The CIE could therefore explain our observed low δ^{13}C values of shells living in ^{13}C-enriched waters. However, an in-depth interpretation of this effect is not possible as during cruise ARKXXVI/1 the parameters needed to calculate $[CO_3^{2-}]$ (pH and total alkalinity of the water samples) were not determined.

As also discussed with respect to the offset in δ^{18}O between coretop and living foraminifera, the age of core top samples can vary in a great range (between modern to 3 ky, with an average of ~ 1 kyr, Simstich et al., 2003). As a result, they may re-

cc BY

flect significantly older environments than the plankton samples. The negative offset in δ^{13}C between the sediment and plankton samples may thus be explained by the surface ocean Suess effect: during the last 100 years the carbon isotope composition of the atmosphere has changed due to the increased anthropogenic combustion of fossil carbon which is extremely negative in δ^{13}C. The δ^{13}C values of the atmospheric CO_2 have decreased by about 1.4 ‰ (Friedli et al., 1986; Francey et al., 1999) and the concurrent shift in the stable carbon isotope composition of ocean surface water is reflected in the decrease of δ^{13}C of recent foraminiferal shells (Bauch et al., 2000). The offset of roughly −1 ‰ in δ^{13}C between the sediment and plankton samples observed both in this study and in that of Bauch et al. (2000) may therefore be explained by the different ages of the carbonate in both sample sets.

6 Conclusions

1. The polar species *Neogloboquadrina pachyderma* (sin.) clearly dominates the foraminiferal species assemblage in the Fram Strait in the early summer. Subpolar *Turborotalita quinqueloba* accounts for only 5–25 %.
2. In the study area both species dwell shallower under the ice cover than in the open ocean. The average depth of calcification of *N. pachyderma* (sin.) lies between 70–150 m water depth, *T. quinqueloba* shows a similar range with 50–120 m water depth.
3. When calculating the average vital effect in the oxygen isotope composition for the whole sampled water column, *N. pachyderma* (sin.) and *T. quinqueloba* show an average offset of about −1.5 ‰ and −3.7 ‰ (respectively) compared to calculated equilibrium calcite values. These vital effects are higher than those determined at the calcification depth only where it is −0.9 ‰ for *N. pachyderma* (sin.) and −3.1 ‰ for *T. quinqueloba*.

4. The $\delta^{13}C_{DIC}$ and the $\delta^{13}C$ values of net-sampled shells show an average offset of −1.6 ‰ and −3.6 ‰ for *N. pachyderma* (sin.) and *T. quinqueloba*, respectively. The discrepancies with earlier published results may suggest the influence of regional variability on the vital effect in $\delta^{13}C$.
5. In the upper ~ 75 m of the water column the $\delta^{13}C_{DIC}$ and the $\delta^{13}C$ of shells of both species show an exactly reverse tendency that might relate to the influence of the "carbonate ion effect" on the carbon isotope incorporation in the tests.
6. The shells of both species collected from the water column yield lower $\delta^{18}O$ and $\delta^{13}C$ values than those from the sediment surface, suggesting that the tests recorded changes in environmental parameters influencing the stable isotope compositions in the past ~ 200–1000 years. The negative offset in $\delta^{18}O$ between the sediment and plankton samples suggests a combined effect of temperature rise and $\delta^{18}O_{water}$-change, while the offset in $\delta^{13}C$ may be explained by the surface ocean Suess effect.

Acknowledgements. The authors wish to thank the captain and crew of RV *Polarstern* and the Alfred Wegener Institute, Helmholtz Centre for Polar and Marine Research in Bremerhaven for support during the cruise ARK XXVI/1. We are indebted to Angelina Kraft for assisting in the deployments of the MultiNet sampler and to Maciej Telesinski for collecting the sediment surface samples for this study. Agnieszka Beszczynska-Möller and Andreas Wisotzki provided the CTD-data for the study. Thanks also go to Hartmut Schulz for kindly providing the low temperature vacuum asher at the University of Tübingen and for his hospitality and technical assistance during the process. This research was conducted with funding of the European Community's 7th Framework Programme FP7 2007/2013, Marie-Curie Actions, under Grant Agreement No. 238111 – CASE ITN. R. F. Spielhagen acknowledges the financial support through the "Akademienprogramm" by the Academy of Sciences, Humanities, and Literature Mainz.

The service charges for this open access publication
have been covered by a Research Centre of the
Helmholtz Association.

References

Bauch, D., Carsens, J., and Wefer, G.: Oxygen isotope composition of living *Neogloboquadrina pachyderma* (sin.) in the Arctic Ocean, Earth Planet. Sc. Lett., 146, 47–58, 1997.

Bauch, D., Carstens, J., Wefer, G., and Thiede, J.: The imprint of anthropogenic CO_2 in the Arctic Ocean: evidence from planktic $\delta^{13}C$ data from water column and sediment surfaces, Deep-Sea Res. Pt. II, 47, 1791–1808, 2000.

Bauch, D., Erlenkeuser, H., Winckler, G., Pavlova, G., and Thiede, J.: Carbon isotopes and habitat of polar planktic foraminifera in the Okhotsk Sea: the “carbonate ion effect” under natural conditions, Mar. Micropaleontol., 45, 83–99, 2002.

Bemis, B. E., Spero, H. J., Bijma, J., and Lea, D. W.: Reevaluation of the oxygen isotopic composition of planktonic foraminifera: experimental results and revised paleotemperature equations, Paleoceanography, 13, 150–160, 1998.

Berberich, D.: Die planktische Foraminifere *Neogloboquadrina pachyderma* (Ehrenberg) im Weddellmeer, Antarktis [The planktonic foraminifera *Neogloboquadrina pachyderma* (Ehrenberg) in the Weddell Sea, Antarctica], Berichte zur Polarforschung (Reports on Polar Research, 195, 1996.

Berger, W. H.: Planktonic foraminifera: selective solution and the lysocline, Mar. Geol., 8, 111–138, 1970.

Beszczynska-Möller, A. and Wisotzki, A.: Physical oceanography during POLARSTERN cruise ARKXXVI/1, Alfred Wegener Institute, Helmholtz Centre for Polar and Marine Research, Bremerhaven, doi:10.1594/PANGAEA.774196, 2012.

Beszczynska-Möller, A., Woodgate, R. A., Lee, C., Melling, H., and Karcher, M.: A synthesis of exchanges through the main oceanic gateways to the Arctic Ocean, in: The Changing Arctic Ocean: Special Issue on the International Polar Year (2007–2009), Oceanography, 24, 82–99, 2011.

Bijma, J., Erez, J., and Hemleben, C.: Lunar and semi-lunar reproductive cycles in some spinose planktonic foraminifers, J. Foramin. Res., 20, 117–127, 1990.

Chierici, M. and Fransson, A.: Calcium carbonate saturation in the surface water of the Arctic Ocean: undersaturation in freshwater influenced shelves, Biogeosciences, 6, 2421–2431, doi:10.5194/bg-6-2421-2009, 2009.

cc BY

Dickson, R. R., Osborn, T. J., Hurrell, J. W., Meincke, J., Blindheim, J., Adlandsvik, B., Vinje, T., Alekseev, G., and Maslowski, W.: The Arctic Ocean response to the North Atlantic Oscillation, J. Climate, 13, 2671–2696, 2000.

Duplessy, J. C.: Isotope studies, Climatic Change, 3, 47–67, 1978.

Duplessy, J. C., Bé, A. W. H., and Blanc, P. L.: Oxygen and carbon isotopic composition and biogeographic distribution of planktonic foraminifera in the Indian Ocean, Palaeogeogr. Palaeocl., 33, 9–46, 1981.

Duplessy, J. C., Labeyrie, L., Arnold, M., Paterne, M., Duprat, J., and van Weering, T. C.: Changes in surface salinity of the North Atlantic Ocean during the last deglaciation, Nature, 358, 485–488, 1992.

Ehrenberg, C. G.: Über die Tiefgrund-Verhältnisse des Oceans am Eingange der Davisstrasse und bei Island (About sea bottom conditions at the mouth of Davis Strait and near Iceland), Monatsbericht der Königlichen Preussischen Akademie der Wissenschaften zu Berlin 1861, 275–315, 1861.

Erez, J. and Luz, B.: Experimental paleotemperature equation for planktonic foraminifera, Geochim. Cosmochim. Ac., 47, 1025–1031, 1983.

Fairbanks, R. G., Wiebe, P. H., and Be, A. W. H.: Vertical distribution and isotopic composition of living planktonic foraminifera in the western North Atlantic, Science, 207, 61–63, 1980.

Fogel, M. L. and Cifuentes, L. A.: Isotope fractionation during primary production, in: Organic Geochemistry, Springer US, 73–98, 1993.

Francey, R. J., Allison, C. E., Etheridge, D. M., Trudinger, C. M., Enting, I. G., Leuenberger, M., Langenfelds, R. L., Michel, E., and Steele, L. P.: A 1000-year high precision record of δ^{13}C in atmospheric CO_2, Tellus B, 51, 170–193, 1999.

Friedli, H., Lötscher, H., Oeschger, H., Siegenthaler, U., and Stauffer, B.: Ice core record of the $^{13}C/^{12}C$ ratio of atmospheric CO_2 in the past two centuries, Nature, 324, 237–238, 1986.

Gillooly, J. F., Brown, J. H., West, G. B., Savage, V. M., and Charnov, E. L.: Effects of size and temperature on metabolic rate, Science, 293, 2248–2251, 2001.

Hecht, A. D.: An ecologic model for test size variation in recent planktonic foraminifera; applications to the fossil record, J. Foramin. Res., 6, 295–311, 1976.

Hemleben, C., Spindler, M., and Anderson, O. R.: Modern Planktonic Foraminifera, Springer, New York, 1989.

Hemmingsen, A. M.: Energy metabolism as related to body size and respiratory surfaces, and its evolution, Rep. Steno Mem. Hosp. Nord. Insulinlab., 9, 1–110, 1960.

cc BY

Jakobsson, M., Mayer, L., Coakley, B., Dowdeswell, J. A., Forbes, S., Fridman, B., Hodnesdal, H., Noormets, R., Pedersen, R., Rebesco, M., Schenke, H. W., Zarayskaya, Y., Accettella, D., Armstrong, A., Anderson, R. M., Bienhoff, P., Camerlenghi, A., Church, I., Edwards, M., Gardner, J. V., Hall, J. K., Hell, B., Hestvik, O., Kristoffersen, Y., Marcussen, C., Mohammad, R., Mosher, D., Nghiem, S. V., Pedrosa, M. T., Travaglini, P. G., and Weatherall, P.: The International Bathymetric Chart of the Arctic Ocean (IBCAO) version 3.0., Geophys. Res. Lett., 39, L12609, doi:10.1029/2012GL052219, 2012.

Johanessen, O. M.: Brief overview of the physical oceanography, in: The Nordic Seas, edited by: Hurdle, B. G., Springer, New York, 103–128, 1986.

Jones, E. P.: Circulation in the Arctic Ocean, Polar Res., 20, 139–146, 2001.

Jonkers, L., Brummer, G.-J. A., Peeters, F. J. C., van Aken, H. M., and De Jong, M. F.: Seasonal stratification, shell flux, and oxygen isotope dynamics of left-coiling *N. pachyderma* (sin.) and *T. quinqueloba* in the western subpolar North Atlantic, Paleoceanography, 25, PA2204, doi:10.1029/2009PA001849, 2010.

Kahn, M. I.: Non-equilibrium oxygen and carbon isotopic fractionation in tests of living planktonic-foraminifera, Oceanol. Acta, 2, 195–208, 1979.

Kellogg, T., Duplessy, J. C., and Shackleton, N.: Planktonic foraminiferal and oxygen isotopic stratigraphy and paleoclimatology of Norwegian Sea deep-sea cores, Boreas, 7, 61–73, 1978.

Kohfeld, K. E., Fairbanks, R. G., Smith, S. L., and Walsh, I. D.: *Neogloboquadrina pachyderma* (sinistral coiling) as paleoceanographic tracers in polar oceans: evidence from Northeast Water Polynya plankton tows, sediment traps, and surface sediments, Paleoceanography, 11, 679–699, 1996.

Lončarić, N., Peeters, F. J. C., Kroon, D., and Brummer, G.-J. A.: Oxygen isotope ecology of recent planktic foraminifera at the central Walvis Ridge (SE Atlantic), Paleoceanography, 21, PA3009, doi:10.1029/2005PA001207, 2006.

McConnaughey, T.: ^{13}C and ^{18}O isotopic disequilibrium in biological carbonates: I. Patterns, Geochim. Cosmochim. Ac., 53, 151–162, 1989.

Meyer, H., Schoenicke, L., Wand, U., Hubberten, H.-W., and Friedrichsen, H.: Isotope studies of hydrogen and oxygen in ground ice – experiences with the equilibration technique, Isot. Environ. Healt. S., 36, 133–149, 2000.

Natland, M. L.: New species of foraminifera from off the west coast of North America and from the later Tertiary of the Los Angeles Basin, Scripps Institute of Oceanography Bulletin Technical Series, 4, 137–164, 1938.

O'Neil, J. R., Clayton, R. N., and Mayeda, T. K.: Oxygen isotope fractionation in divalent metal carbonates, J. Chem. Phys., 51, 5547–5558, 1969.

Pados, T. and Spielhagen, R. F.: Species distribution and depth habitat of recent planktic foraminifera in the Fram Strait (Arctic Ocean), Polar Res., 33, 22483, doi:10.34027/polar.v33.22483, 2014.

Peterson, B. J., Holmes, R. M., McClelland, J. W., Vörösmarty, C. J., Lammers, R. B., Shiklomanov, A. I., and Rahmstorf, S.: Increasing river discharge to the Arctic Ocean, Science, 298, 2171–2173, 2002.

Romanek, C. S., Grossman, E. L., and Morse, J. W.: Carbon isotopic fractionation in synthetic aragonite and calcite: effects of temperature and precipitation rate, Geochim. Cosmochim. Ac., 56, 419–430, 1992.

Rudels, B., Friedrich, H. J., and Quadfasel, D.: The Arctic Circumpolar Boundary Current, Deep-Sea Res. Pt. II, 46, 1023–1062, 1999.

Rudels, B., Meyer, R., Fahrbach, E., Ivanov, V. V., Østerhus, S., Quadfasel, D., Schauer, U., Tverberg, V., and Woodgate, R. A.: Water mass distribution in Fram Strait and over the Yermak Plateau in summer 1997, Ann. Geophys., 18, 687–705, doi:10.1007/s00585-000-0687-5, 2000.

Schiebel, R. and Hemleben, C.: Modern planktic foraminifera, Palaeontol. Z., 79, 135–148, 2005.

Schmidt, G. A. and Mulitza, S.: Global calibration of ecological models for planktic foraminifera from coretop carbonate oxygen-18, Mar. Micropaleontol., 44, 125–140, 2002.

Serreze, M. C., Walsh, J. E., Chapin III, F. S., Osterkamp, T., Dyurgerov, M., Romanovsky, V., Oechel, W. C., Morison, J., Zhang, T., and Barry, R. G.: Observational evidence of recent change in the northern high latitude environment, Climatic Change, 46, 159–207, 2000.

Shackleton, N. J., Wiseman, J. D. H., and Buckley, H. A.: Non-equilibrium isotopic fractionation between seawater and planktonic foraminiferal tests, Nature, 242, 177–179, 1973.

Simstich, J., Sarnthein, M., and Erlenkeuser, H.: Paired δ^{18}O signals of *Neogloboquadrina pachyderma* (s) and *Turborotalita quinqueloba* show thermal stratification structure in the Nordic Seas, Mar. Micropaleontol., 48, 107–125, 2003.

Spero, H. J.: Do planktic foraminifera accurately record shifts in the carbon isotopic composition of seawater ΣCO_2?, Mar. Micropaleontol., 19, 275–285, 1992.

Spero, H. J. and Deniro, M. J.: The influence of symbiont photosynthesis on the $\delta^{18}O$ and $\delta^{13}C$ values of planktonic foraminiferal shell calcite, Symbiosis, 4, 213–228, 1987.

Spero, H. J., Bijma, J., Lea, D. W., and Bemis, B. E.: Effect of seawater carbonate concentration on foraminiferal carbon and oxygen isotopes, Nature, 390, 497–500, 1997.

Spielhagen, R. F., Werner, K., Sorensen, S. A., Zamelczyk, K., Kandiano, E., Budeus, G., Husum, K., Marchitto, T. M., and Hald, M.: Enhanced modern heat transfer to the Arctic by warm Atlantic water, Science, 331, 450–453, 2011.

Vergnaud Grazzini, C.: Non-equilibrium isotopic compositions of shells of planktonic foraminifera in the Mediterranean Sea, Paleogeogr. Paleocl., 20, 263–276, 1976.

Volkmann, R.: Planktic foraminifers in the outer Laptev Sea and the Fram Strait – modern distribution and ecology, J. Foramin. Res., 30, 157–176, 2000.

Volkmann, R. and Mensch, M.: Stable isotope composition ($\delta^{18}O$, $\delta^{13}C$) of living planktic foraminifers in the outer Laptev Sea and the Fram Strait, Mar. Micropaleontol., 42, 163–188, 2001.

von Gyldenfeldt, A.-B., Carstens, J., and Meincke, J.: Estimation of the catchment area of a sediment trap by means of current meters and foraminiferal tests, Deep-Sea Res. Pt. II, 47, 1701–1717, 2000.

Zhang, J., Rothrock, D. A., and Steele, M.: Warming of the Arctic Ocean by a strengthened Atlantic inflow: model results, Geophys. Res. Lett., 25, 1745–1748, 1998.

Table 1. List of the stations sampled during cruise ARKXXVI/1 in June/July 2011.

Station	Latitude	Longitude	Water depth	Date	Ice cover
PS78-19	78°49.84′ N	6°0.69′ E	2464 m	25.06.11	no
PS78-25	78°49.962′ N	7°0.077′ E	1465 m	26.06.11	no
PS78-35	78°49.772′ N	3°58.380′ E	2335 m	28.06.11	no
PS78-39	78°50.09′ N	1°54.56′ E	2554 m	28.06.11	no
PS78-44	78°49.972′ N	0°4.630′ E	2636 m	29.06.11	no
PS78-54	78°50.02′ N	2°0.21′ W	2714 m	01.07.11	ice margin
PS78-71	78°49.66′ N	5°20.99′ W	684 m	04.07.11	ice covered
PS78-75	78°49.74′ N	3°55.44′ W	1978 m	04.07.11	ice covered
PS78-87	78°50.44′ N	3°0.19′ E	2454 m	06.07.11	no
PS78-127	78°49.84′ N	8°1.33′ E	1019 m	10.07.11	no

Table 2. $\delta^{18}O$, $\delta^{13}C$ and equilibrium calcite values in the upper 500 m of the water column.

Station	Depth (m)	$\delta^{18}O$ (‰ SMOW)	$\delta^{13}C$ (‰ PDB)	Equ. calc.
PS78-19	0	0.29	1.63	2.90
	25	0.38	1.71	3.01
	50	0.4	1.39	3.32
	75	0.34	0.92	3.44
	100	0.21	0.66	3.33
	125		0.95	
	150	0.28	1.06	3.49
	200	0.31	0.84	3.55
	250	0.21		3.50
	300	0.31	0.95	3.66
	400	0.23	1.10	3.77
	500	0.27	1.06	3.91
PS78-25	0	0.32	0.89	2.70
	25	0.37	0.92	2.73
	50	0.33	0.96	3.24
	75	0.3	0.98	3.29
	100	0.31	0.86	3.36
	125	0.3	0.83	3.44
	150	0.28	0.97	3.47
	200	0.29	0.90	3.50
	250			
	300	0.26	0.95	3.53
	400	0.25	0.99	3.70
	500	0.25	0.94	3.94
PS78-35	0	−0.98	1.30	3.06
	25	−0.46	1.30	3.99
	50	0.09	1.03	4.26
	75	0.23	0.96	3.62
	100	0.29	0.70	3.53
	125	0.37	0.73	3.65
	150	0.29	0.99	3.63
	200	0.33	1.05	3.82
	250			
	300	0.33	1.01	3.81
	400	0.23	1.07	3.82
	500	0.29	1.01	4.00
PS78-39	0	−0.29	1.50	3.92
	25	−0.25	1.31	4.27
	50	0.06	1.21	4.64
	75	0.14	1.11	3.99
	100	0.17	0.97	4.02
	125	0.22	1.05	3.82
	150	0.25	1.13	3.67
	200	0.36	1.01	3.87
	250			
	300	0.28	0.82	3.76
	400	0.29	0.79	3.71
	500	0.28	1.09	3.80

Title Page
Abstract | Introduction
Conclusions | References
Tables | Figures
◀ ▶
Back | Close
Full Screen / Esc
Printer-friendly Version
Interactive Discussion

CC BY

Table 2. Continued.

Station	Depth (m)	δ^{18}O (‰ SMOW)	δ^{13}C (‰ PDB)	Equ. calc.
PS78-44	0	0.25	1.39	2.73
	25	0.38	1.16	3.03
	50	0.38	1.01	3.14
	75	0.3	0.88	3.19
	100	0.37	0.89	3.40
	125	0.38	0.98	3.48
	150	0.31	0.96	3.45
	200	0.29	1.19	3.47
	250			
	300	0.28	0.88	3.60
	400	0.35	0.98	3.79
	500	0.28	1.14	3.89
PS78-54	0	0.33	1.68	4.41
	25	0.41	1.61	4.69
	50	0.37	0.94	3.06
	75	0.32	0.95	3.21
	100	0.37	1.06	3.38
	125	0.36	0.94	3.44
	150	0.36	1.10	3.49
	200	0.25	1.09	3.46
	250			
	300	0.21	0.90	3.49
	400	0.36	1.04	3.72
	500	0.3	0.87	3.77
PS78-71	0	−2.63	1.49	1.67
	25	−2.4	1.50	2.15
	50	−2.18	1.23	2.38
	75	−1.41	1.12	3.13
	100	−1	1.11	3.49
	125	−0.52	1.02	3.98
	150	−0.25	1.09	4.24
	200	0.04	1.13	4.15
	250			
	300	0.36	0.94	4.13
	400	0.37	0.95	4.07
	500	0.4	1.18	4.34
PS78-75	0	−2.2	1.34	2.31
	25	−1.85	0.96	2.70
	50	−1.2	1.15	3.34
	75	−0.51	1.10	3.94
	100	−0.27	1.11	4.05
	125	−0.09	0.91	4.16
	150	0.21	0.86	4.24
	200	0.36	0.91	3.34
	250			
	300	0.37	1.01	3.46
	400	0.34	0.87	3.56
	500	0.36	0.99	4.19

Title Page
Abstract | Introduction
Conclusions | References
Tables | Figures
◀I | ▶I
◀ | ▶
Back | Close
Full Screen / Esc
Printer-friendly Version
Interactive Discussion

Table 2. Continued.

Station	Depth (m)	δ^{18}O (‰ SMOW)	δ^{13}C (‰ PDB)	Equ. calc.
PS78-87	0	0.31	1.54	2.58
	25	0.38	1.20	2.51
	50	0.35	1.08	2.94
	75	0.3	1.02	3.02
	100	0.36	0.64	3.19
	125	0.35	0.70	3.27
	150	0.37	0.69	3.38
	200	0.29	0.86	3.46
	250			
	300	0.36	0.79	3.67
	400	0.33	0.64	3.74
	500	0.37	0.87	3.87
PS78-127	0	0.34	1.64	2.60
	25	0.49	1.31	2.64
	50	0.4	0.95	2.91
	75	0.21	0.85	2.76
	100	0.38	0.87	2.96
	125	0.32	0.93	2.94
	150	0.36	0.88	3.03
	200	0.34	0.94	3.07
	250			
	300	0.28	0.96	3.22
	400	0.32	1.00	3.40
	500	0.3	1.02	3.49

CC BY

Table 3. δ^{18}O and δ^{13}C values of *N. pachyderma* (sin.) (*N.p.* (sin.)) and *T. quinqueloba* (*T.q.*) from sediment surface samples.

	δ^{18}O (‰ PDB)		δ^{13}C (‰ PDB)	
Station	*N. p.* (sin.)	*T. q.*	*N. p.* (sin.)	*T. q.*
PS78-19	3.17	2.56	0.44	−1.10
PS78-25	2.84	2.05	0.15	−1.28
PS78-35	3.36	2.70	0.66	−1.05
PS78-39	3.31	2.53	0.61	−1.20
PS78-44	3.35	2.98	0.49	−1.09
PS78-54	3.44	3.08	0.75	−0.59
PS78-71	3.32		0.50	
PS78-75	3.57	3.00	0.72	−0.67
PS78-87	3.36	2.75	0.58	−1.02
PS78-127	2.71		0.09	

Table 4. δ^{18}O and δ^{13}C values of *N. pachyderma* (sin.) (*N. p.* (sin.)) and *T. quinqueloba* (*T. q.*) from plankton tows.

		δ^{18}O (‰ PDB)		δ^{13}C (‰ PDB)	
Station	Depth (m)	*N. p.* (sin.)	*T. q.*	*N. p.* (sin.)	*T. q.*
PS78-19	0–50	2.38		−0.99	
	50–100	2.69	1.96	−0.40	−1.64
	100–200	2.82	1.81	−0.38	−1.88
	200–300	2.36		−0.74	
	300–500	2.67		−0.78	
PS78-25	0–50	2.40		−0.78	
	50–100	2.55	−2.85	−0.37	−4.25
	100–200	2.51	1.64	−0.10	−1.72
	200–300	1.98		−1.40	
	300–500	2.56	0.31	−0.43	−2.50
PS78-35	0–50	2.32	−5.54	−0.89	−6.13
	50–100	3.08	−5.57	−0.28	−6.03
	100–200	3.00	2.25	−0.15	−1.68
	200–300	2.95		−0.16	
	300–500	2.88		−0.44	
PS78-39	0–50	3.25	−4.99	−0.19	−5.79
	50–100	3.25	−1.36	−0.13	−3.61
	100–200	3.34	1.57	0.08	−1.99
	200–300	3.34		0.03	
	300–500	2.32		−0.75	
PS78-44	0–50	2.58	−7.35	−0.60	−7.86
	50–100	2.64		−0.44	
	100–200	3.01	2.13	−0.10	−1.44
	200–300	2.86	0.41	−0.25	−2.46
	300–500	2.65	−0.51	−0.83	−5.78
PS78-54	0–50	2.77	−0.86	−0.62	−5.96
	50–100	2.75	2.46	−0.21	−1.22
	100–200	2.83	2.20	−0.21	−1.56
	200–300	2.69	1.59	−0.24	−2.57
	300–500	2.61	2.18	−0.28	−1.52
PS78-71	0–50	0.99		−0.63	
	50–100	1.86	1.72	−0.14	−1.78
	100–200	1.80	−1.93	−1.04	−3.84
	200–300	2.89	0.85	−0.15	−2.30
	300–500	2.12		−0.50	
PS78-75	0–50	−2.94		−4.14	
	50–100	1.36	−2.72	−0.79	−4.00
	100–200	0.93		−0.69	
	200–300	0.56		−1.38	
	300–500				
PS78-87	0–50	−1.54		−2.14	
	50–100	1.87	0.25	−0.43	−3.54
	100–200	1.89	0.25	−1.37	−2.22
	200–300	0.23		−1.88	
	300–500	−2.56		−4.38	
PS78-127	0–50	1.07	−5.01	−2.59	−7.79
	50–100	2.80	1.99	−0.48	−1.72
	100–200	2.06	2.39	−0.98	−1.51
	200–300	2.08	2.42	−1.02	−1.54
	300–500	2.16	1.90	−1.06	−1.76

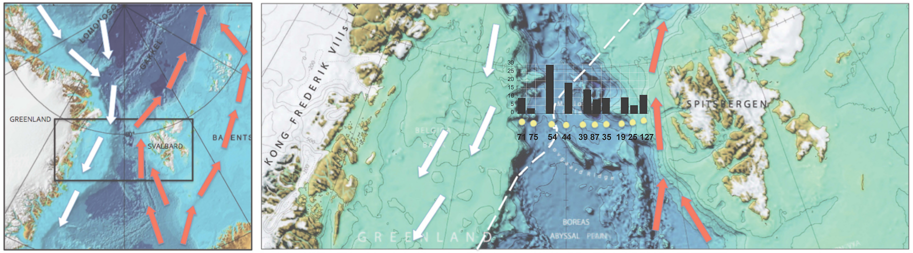

Figure 1. Map and schematic surface ocean circulation of the study area (red arrows: West Spitsbergen Current, white arrows: East Greenland Current). The enlarged part shows the sampled stations (yellow dots). Bars represent absolute abundances (ind./m^3 water) of planktic foraminifera in the upper 500 m of the water column along the transect at 78°50′ N across the Fram Strait. The white dashed line shows the position of the sea ice margin during the sampling period (shipboard observation and satellite data from the US National Oceanic and Atmospheric Administration). Map source: the International Bathymetric Chart of the Southern Ocean (Jakobsson et al., 2012).

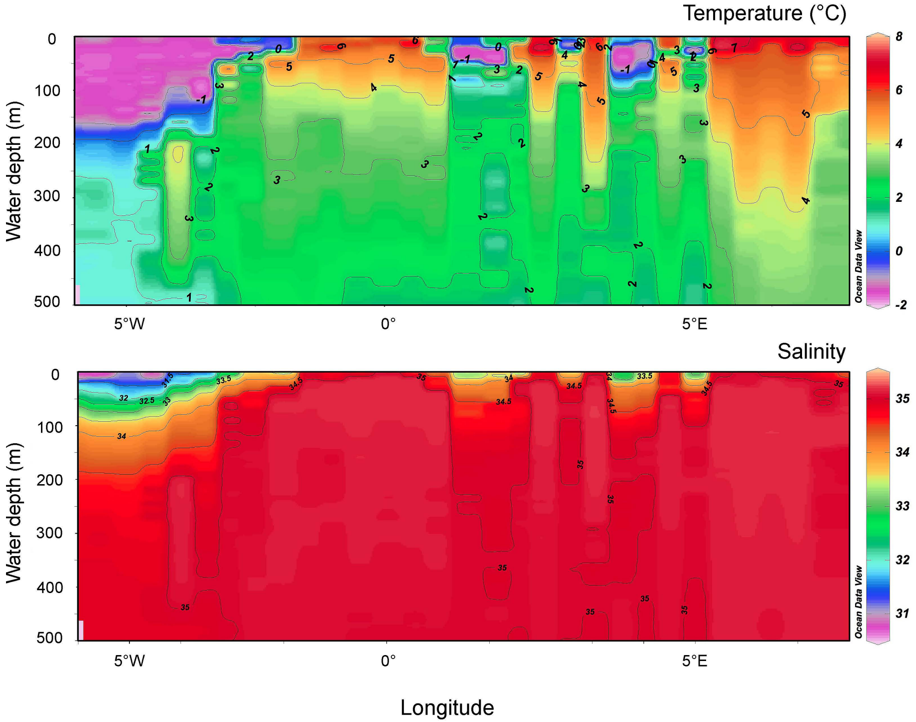

Figure 2. Temperature and salinity of the water column in the upper 500 m along a transect at 78°50′ N across the Fram Strait. Data obtained by conductivity–temperature–density (CTD) measurements during the expedition ARK XXVI/1 (Beszczynska-Möller and Wisotzki, 2012). The figure comprises data obtained from 30 CTD stations, equally distributed along the transect.

Title Page
Abstract
Introduction
Conclusions
References
Tables
Figures
I◀
▶I
◀
▶
Back
Close
Full Screen / Esc
Printer-friendly Version
Interactive Discussion

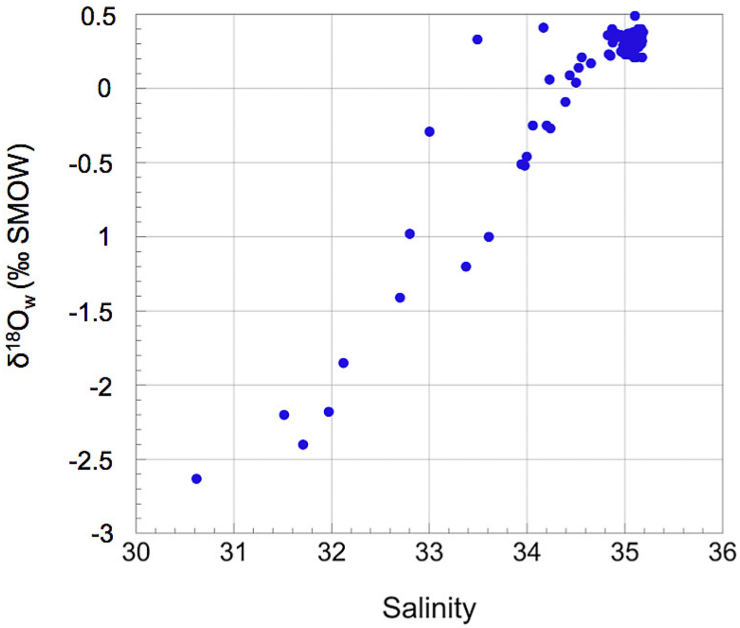

Figure 3. δ^{18}O (‰ SMOW) values of the upper 500 m of the water column vs. salinities (PSU) for the sampled transect at 78°50′ N across the Fram Strait.

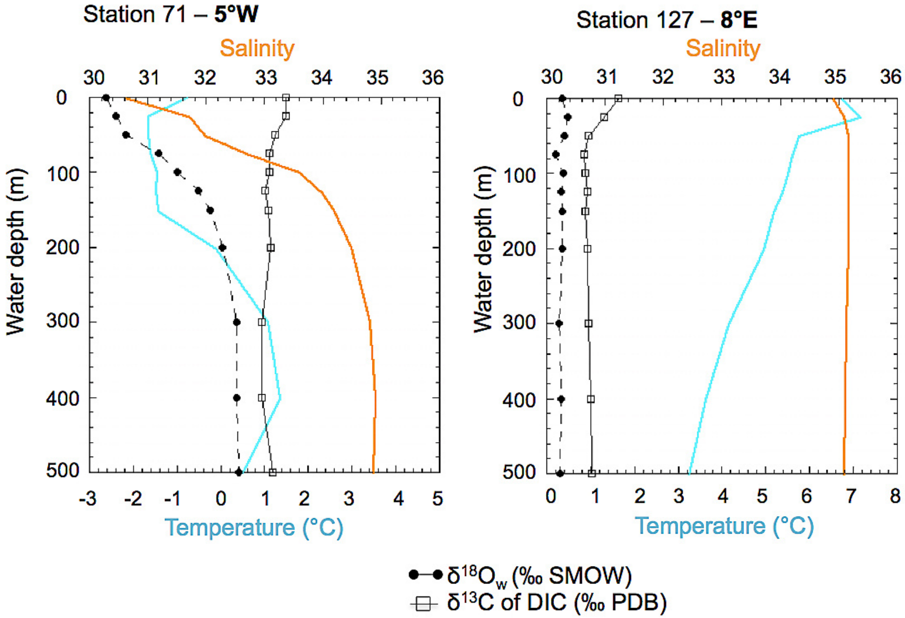

Figure 4. Salinity, temperature, δ^{18}O (‰ SMOW) and $\delta^{13}C_{DIC}$ (‰ PDB) profiles of the upper 500 m of the water column from the westernmost and easternmost stations sampled along a transect at 78°50′ N across the Fram Strait.

Title Page
Abstract | Introduction
Conclusions | References
Tables | Figures
◀| |▶
◀ ▶
Back | Close
Full Screen / Esc
Printer-friendly Version
Interactive Discussion

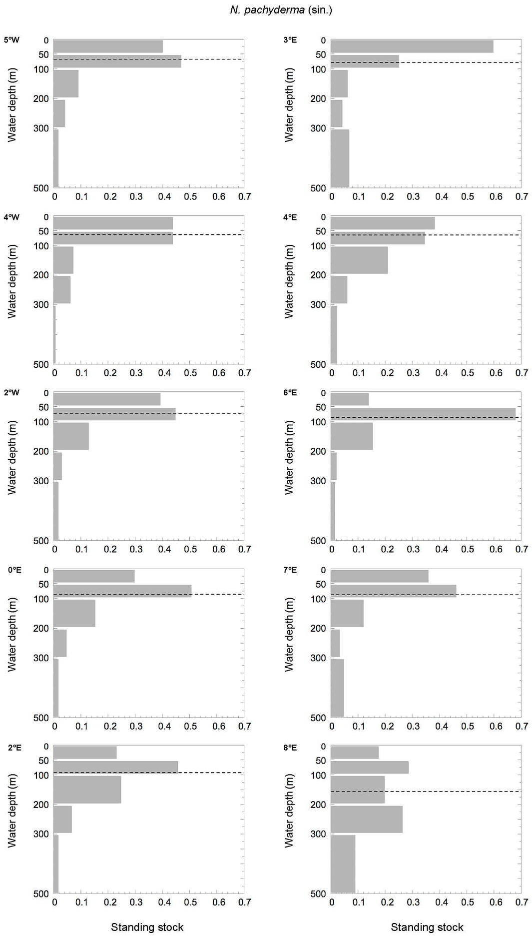

Figure 5. Standing stock of *N. pachyderma* (sin.) for each sampling interval. The black dashed line indicates the average depth of calcification (calculated from the standing stock).

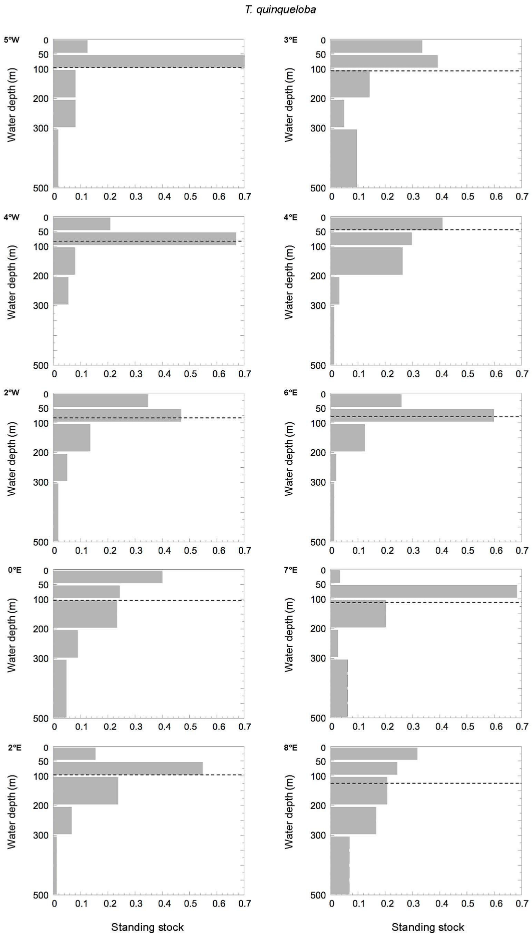

Figure 6. Standing stock of *T. quinqueloba* for each sampling interval. The black dashed line indicates the average depth of calcification (calculated from the standing stock).

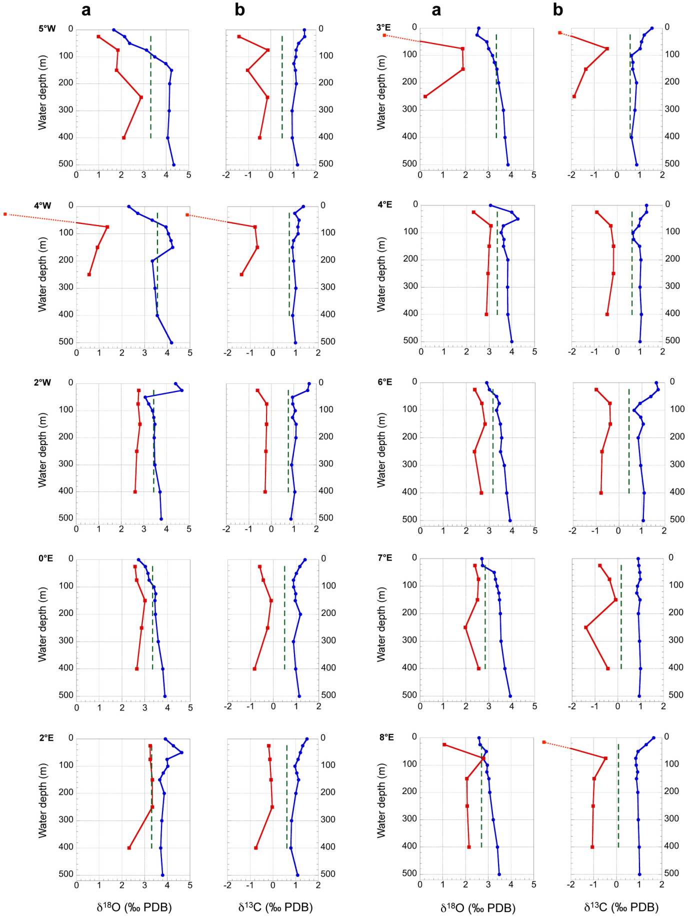

Figure 7. (a) δ^{18}O and **(b)** δ^{13}C values of *N. pachyderma* (sin.) from the water column (red squares) and from the sediment surface (green dashed line). The blue dots indicate **(a)** the equilibrium calcite and **(b)** the δ^{13}C$_{\text{DIC}}$ profile of the water column.

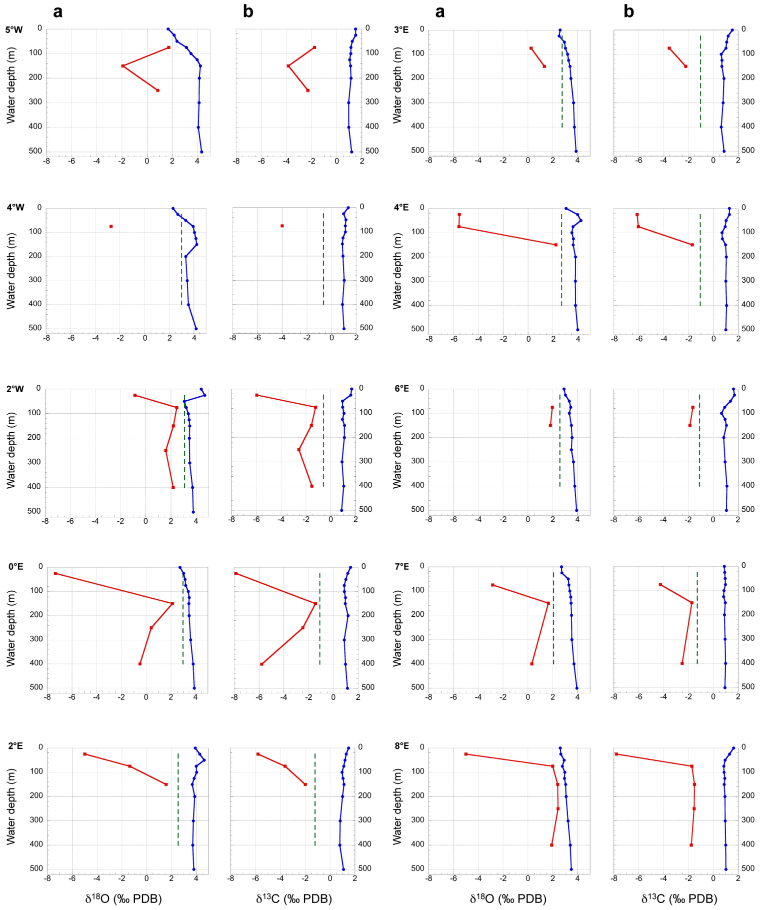

Figure 8. (a) δ^{18}O and **(b)** δ^{13}C values of *T. quinqueloba* from the water column (red squares) and from the sediment surface (green dashed line). The blue dots indicate **(a)** the equilibrium calcite and **(b)** the $\delta^{13}C_{DIC}$ profile of the water column.